Actin Polymerization in Cellular Oxidant Injury[1]

Daniel B. Hinshaw,[2] Jeanne M. Burger, Theodore F. Beals, Barbara C. Armstrong,*
and Paul A. Hyslop†

*Departments of Surgery and Pathology, VA Medical Center and University of Michigan, Ann Arbor, Michigan; *VA Medical
Center, Richmond, Virginia; and †Department of CNS Pharmacology, Lilly Research Laboratories, Indianapolis, Indiana*

**Microfilaments undergo an ATP-dependent disruption
into shortened bundles following cellular exposure to
oxidants. This phenomenon does not require a net change
in the amount of polymerized actin. However, increased
amounts of polymerized actin have been detected in ox-
idant-injured cells and it was the purpose of this study
to determine the conditions under which the actin poly-
merization may occur. Utilizing the formation of oxidized
glutathione (GSSG) as an indicator of cellular sulfhy-
dryl oxidation, conditions were chosen to accentuate
sulfhydryl oxidation within the target P388D₁ cell line
following exposure to the oxidants, H₂O₂ and diamide.
Using the DNase I and flow cytometric assays of actin
polymerization, significant polymerization of actin was
detected only under conditions in which sulfhydryl oxi-
dation occurred after exposure to the two oxidizing
agents. Greater sulfhydryl oxidation early in the course
of injury was associated with a greater rate and extent
of actin polymerization in the injured cells. Experiments
with cells depleted of glutathione (GSH) demonstrated
that neither loss of GSH nor absolute levels of GSSG
formed during oxidant exposure were responsible for the
polymerization of actin. The data presented are consis-
tent with the hypothesis that oxidizing conditions which
induce significant sulfhydryl oxidation in target cells are
correlated with assembly of polymerized actin and that
this represents a process which is distinct and separate
from the ATP-dependent gross disruption of microfila-
ments.** © 1991 Academic Press, Inc.

Dramatic changes in microfilament organization occur
following cellular exposure to oxidants (1, 2). Microfila-
ments undergo disruption into shortened bundles after

exposure to H₂O₂. The bundles appear at an ultrastruc-
tural level to be identical to bundles which develop in
cells experiencing metabolic inhibition (3, 4). Both met-
abolic inhibition and oxidant exposure result in reduction
of cellular ATP levels (5, 6) which correlates well with
the disruption of microfilament morphology. Following
release from metabolic inhibition with partial recovery of
ATP levels, normal microfilament architecture returns
(4). The disruption of microfilaments into bundles which
occurs in association with reduced levels of ATP does not
require a change in the amount of polymerized (F) actin
present (3).

Increases in F actin can occur following oxidant ex-
posure to cells (1). It is not clear, however, what conditions
must be present for actin polymerization to occur in ox-
idant-injured cells and how these conditions may differ
from those which are associated with the ATP-dependent
changes in gross microfilament morphology.

Oxidation of GSH and other cellular sulfhydryls in-
cluding S-S cross-linking of cytoskeletal proteins is known
to occur following oxidant injury (1, 7–10). The oxidation
of GSH to GSSG has been correlated with alterations in
cell surface morphology (e.g., blebbing of the plasma
membrane) (11), inhibition of microtubule assembly in
polymorphonuclear leukocytes (PMN)[3] (12, 13), enhanced
tyrosinolation of tubulin in PMN (14), and disruption of
cell–cell adherence with condensation of microfilaments
in corneal endothelial cells (15). Platelets depleted of GSH
exhibit increased sensitivity to the sulfhydryl oxidizing
agent diamide, with profound effects on cytoskeletal pro-
teins and the aggregation response (16). The hexose
monophosphate (HMP) shunt is activated several-fold
over resting levels of activity in P388D₁ cells following
exposure to H₂O₂ (7). Glucose deprivation at the time of

---

[3] Abbreviations used: BSO, buthionine sulfoximine; MGB, modified
Gey's buffer; DTNB, 5,5′dithiobis 2-nitrobenzoic acid; PMSF, phenyl-
methylsulfonyl fluoride; DTT, dithiothreitol; EGTA, ethylene glycol
bis(β-aminoethyl ether) N,N′-tetraacetic acid; NEM, N-ethylmaleimide;
HMP, hexose monophosphate; PMN, polymorphonuclear leukocytes.

oxidant exposure is associated with considerably more oxidation of cellular sulfhydryls, particularly GSH, than when glucose is present (7). We hypothesized that sulfhydryl oxidation may be responsible for the polymerization of actin induced by oxidants in P388D₁ cells. The experiments described here were designed to examine the effect of conditions which would vary the degree of oxidation of cellular sulfhydryls on the state of actin within cells exposed to the potent sulfhydryl oxidizing agents, H_2O_2 and diamide. The conditions promoting sulfhydryl oxidation were established using the formation of GSSG as an indication of the presence of sulfhydryl oxidation in the target cells. Additional studies in which cells were depleted of GSH prior to oxidant exposure examined the dependence of the oxidant-induced changes in actin on absolute changes in the levels of GSH and GSSG. The P388D₁ cell line was chosen for this study because of the extensive information available concerning its response to oxidants.

MATERIALS AND METHODS

Cells and Culture

The P388D₁ murine cell line (a gift of R. Schreiber, Scripps Clinic and Research Foundation) was cultured as previously described (3). The cells have some macrophage-like properties (IL-1 secretion). A few experiments in this study were performed with P388D₁ cells purchased from the American Type Culture Collection (ATCC), Rockville, MD (see Table I). In some experiments, glutathione synthesis was inhibited by culturing the cells for 18 h in the presence of 200 μM buthionine sulfoximine (BSO), an inhibitor of γ-glutamyl cysteine synthetase (17, 18). The BSO was made up in modified Gey's buffer (MGB) as a 20 mM stock solution and filter sterilized prior to addition to the culture media.

Cell injury at 37°C in a shaking water bath was initiated by addition of a single bolus of the appropriate dilution of reagent grade hydrogen peroxide (H_2O_2, Fisher Scientific) or diamide (Sigma) to the cells. In some of the experiments in which changes in actin and ATP were measured, the buffer was replaced with MGB to which glucose was not added 5 min prior to addition of the oxidant. Controls received equal volumes of MGB without H_2O_2 or diamide.

Glutathione Measurements

Total glutathione (GSH) and oxidized glutathione (GSSG) were measured using standard methods (19, 20). Briefly, 5×10^6 cells were centrifuged for 30 s in a microcentrifuge, the supernatant removed and the pellet deproteinized with 200 μl 2.5% sulfosalicylic acid in 0.2% Triton X-100. After another centrifugation, 100 μl of supernatant was incubated with 2 μl 2-vinylpyridine in 10 μl of 1 M Tris base for 50 min at room temperature for the determination of GSSG. Total GSH and GSSG were determined in plastic cuvettes using 25-μl samples for total GSH and 50-μl samples for GSSG after addition of 500 μl 0.3 mM 5,5′dithiobis 2-nitrobenzoic acid (DTNB), 500 μl 0.4 mM NADPH containing 0.12 U glutathione reductase and 500 μl phosphate/imidazole buffer, pH 7.2. The difference in optical density at 412 nm was read on a spectrophotometer.

Assays of Actin Polymerization

1. DNase I assay. The DNase I assay of Blikstad et al. (21) as described by Howard and Meyer (22) and previously modified (3) was used. DNA substrate for the assay was prepared as follows: 80 μg/ml calf thymus DNA (type 1, Sigma) was added to 0.1 M Tris–HCl, 4 mM

$MgSO_4$ and 1.8 mM $CaCl_2$ (pH 7.5). The DNA solution was stirred for 24–48 h and then filtered. DNase I was prepared as a stock solution: 10 mg/ml DNase I (Sigma type 3 bovine pancreas) was added to 0.25 M Tris–HCl, 5 mM $MgCl_2$, 2 mM $CaCl_2$, 1 mM NaN_3, and 0.1 mM PMSF (phenylmethylsulfonyl fluoride), pH 7.5, and kept at 4°C. Working solutions of the enzyme were prepared by diluting the stock solution 1:100 (100 μg/ml) in 20 mM imidazole, 30 mM NaCl, and 15% glycerol, pH 7.5, and were kept on ice throughout the experiment.

Baseline determination of DNase activity was done using 10 μl (1 μg) DNase solution added to 3 ml DNA solution. Absorbance at 260 nm at 30°C was measured on a LKB Model 4050 spectrophotometer. The slope of enzyme activity from experiment to experiment varied within the range of 0.07–0.08 O.D. units/min. Standard curves of inhibition of DNase I activity by actin were generated in the absence and presence of guanidine HCl (20 μl of a solution containing 1.5 M guanidine HCl, 1 M $NaCH_2CO_2$, 1 mM $CaCl_2$, 1 mM ATP, and 20 mM Tris–HCl, pH 7.5). Actin (Sigma, from bovine muscle) used to inhibit DNase I activity, produced linear inhibition between 30–70% of DNase activity corresponding to a range of 0.4–2.0 μg actin with 1 μg DNase I. H_2O_2 exposure of G actin to be used for the standard curve of DNase I inhibition did not affect its ability to inhibit DNase I.

Actin was measured in P388D₁ cells after resuspension of cell samples at 2×10^7 cells/ml in a lysate solution containing 2 mM $MgCl_2$, 2 mM EGTA, 0.2 mM ATP, 0.5 mM dithiothreitol (DTT), 1% Triton X-100, and 5 mM PMSF in Hanks' buffered salt solution. G-actin was measured by addition of 3 ml of DNA solution to 10 μl DNase I solution and 10–20 μl of cell lysate. Total actin was measured by initially incubating 20 μl of lysate with 20 μl of the guanidine HCl solution on ice for 20 min after brief vortexing. Three milliliters of DNA solution was then added to the 40-μl lysate–guanidine mixture and 10 μl DNase I. Data were expressed as G-actin as a percentage of total actin. Oxidizing conditions did not affect the measurement of total actin in these experiments (see example in discussion).

2. Flow cytometric assay. Oxidant-induced increases in cellular F actin were also measured directly with the flow cytometric assay of Howard and Meyer (1, 22). Cells (1×10^6) (0.5 ml of cell suspension) were centrifuged in a microcentrifuge (Eppendorf) at half-maximal speed for 10–20 s. The pellet was resuspended in 0.45 ml of MGB and combined with 0.05 ml of a solution made up of equal aliquots of 3.3 μM NBD–phallacidin (Molecular Probes, Junction City, Oregon) and 1 mg/ml lysophosphatidyl choline (Sigma) in 37% phosphate-buffered formalin. Samples were then incubated at 37°C for at least 10 min. Stained samples were stable for at least a week after staining when left unwashed and in the dark.

NBD–phallacidin staining of F actin was demonstrated on a flow cytometer (either a FACscan, Becton–Dickinson, Mountain View, CA or Ortho Cytofluorograf) with fluorescence excitation at 488 nm and emission through a 530-nm band pass filter. Fluorescence, forward angle, and right-angle light scatter of 10,000 cells per sample was accumulated in list mode using the Consort 30 or Ortho software. Data presented represent populations of single cells gated to exclude small debris and any large aggregates confirmed by forward angle scatter analysis. Comparisons were then made on the basis of differences in mean fluorescence channel number between the fluorescence histograms of experimental samples and the control.

ATP Measurements

Cellular ATP levels were measured by the luciferase–luciferin method of Stanley and Williams (23) as adapted for use with the P388D₁ cells (5) with the following modifications. The luciferase–luciferin (Sigma No. L0633) was reconstituted at 40 mg/ml in sterile water and diluted 1:50 in a buffer containing 1% bovine serum albumin, 20 mM glycine, and 2 mM EDTA, pH 8.0. Measurements were performed in a LKB Model 1251 automated luminometer.

Statistics

Statistical analysis of DNase I measurements of actin polymerization and ATP measurements were performed using repeated measures analysis of variance. GSH measurements were analyzed using pairwise t tests. Data have been expressed as the mean ± standard deviation with $P < 0.05$ being considered significant.

RESULTS

GSH Oxidation within P388D₁ Cells

Based on earlier experience with P388D₁ cells (7), we chose to monitor formation of GSSG in relation to total GSH equivalents as an indicator of cellular sulfhydryl oxidation. Experimental conditions were chosen which produced rapid (within 5 min) oxidation of at least 50% of cellular GSH equivalents to GSSG after exposure to the two different oxidants, H_2O_2 and diamide (Table I). Cellular oxidant exposure was associated with massive (>50%) GSH oxidation to GSSG only when the cells were deprived of glucose prior to oxidant addition. Exposure to 5 mM H_2O_2 with glucose present was associated at 5 min with only 5.6% oxidation of GSH to GSSG compared to 51.3% when glucose was absent. Diamide was approximately 50-fold more potent than H_2O_2 in terms of its ability to oxidize GSH to GSSG in the absence of glucose. However, the same concentration of diamide (100 μM) in the presence of glucose produced no detectable GSSG over 1 h whereas 5 mM H_2O_2 in the presence of glucose oxidized almost 17% of cellular GSH to GSSG over 1 h. This difference may reflect differences in how the two oxidants interact with targets in the cell. In contrast to the steady increase in GSSG in H_2O_2-treated cells when glucose was

present, GSSG levels decreased by 1 h in cells exposed to H_2O_2 in the absence of glucose. Although the difference in actual GSSG content of cells after 5 min exposure to H_2O_2 was significantly ($P < 0.0001$) different as a function of the presence or absence of glucose, this difference disappeared by 60 min as the actual levels of GSSG became almost identical (Table I). No GSSG was detected in either the plus-glucose control or the minus-glucose control. Exposure of the cells to either oxidant in the absence of glucose was also associated with a very rapid loss ($P < 0.01$) of total GSH equivalents which progressed over the 60 min. Total GSH levels were reduced in cells exposed to H_2O_2 in the presence of glucose but to a much lesser degree than that seen in the absence of glucose ($P < 0.001$). Thus, three of the conditions in Table I exhibited measurable formation of GSSG which was associated with reduction of total GSH equivalents and three did not.

GSH Oxidation and Actin

The effect of conditions which induced rapid and extensive oxidation of GSH on the state of actin within P388D₁ cells was then examined. Using the DNase I inhibition assay for G-actin, actin polymerization in P388D₁ cells was measured over a 60-min time course of exposure to 5 mM H_2O_2 or 100 μM diamide with or without glucose present (Fig. 1). Experimental conditions which led to the formation of GSSG (Table I) were associated with significant ($P < 0.05$) decreases in G-actin as a percentage of total actin (actin polymerization). There was significantly more actin polymerized in cells in which large amounts of GSSG had formed early in the 60-min time

TABLE I

Effect of Glucose Depletion and Oxidant Exposure on GSH/GSSG in P388D₁ Cells

	Control + glucose	Control − glucose	5 mM H_2O_2 + glucose	5 mM H_2O_2 − glucose	Diamide 100 μM + glucose	Diamide 100 μM − glucose
5 minutes						
Total GSH[a]	2.15 ± 0.42	1.75 ± 0.33	1.96 ± 0.38	1.17 ± 0.41	6.02 ± 0.89[b]	0.81 ± 0.28
GSSG[a]	c	c	0.11 ± 0.05	0.60 ± 0.12	c	0.57 ± 0.21
GSSG (% total GSH)	c	c	5.6%	51.3%	c	70.4%
60 minutes						
Total GSH[a]	2.36 ± 0.49	1.85 ± 0.48	1.61 ± 0.39	0.86 ± 0.31	5.16 ± 0.72[b]	0.39 ± 0.16
GSSG[a]	c	c	0.27 ± 0.10	0.24 ± 0.12	c	0.27 ± 0.15
GSSG (% total GSH)	c	c	16.8%	27.9%	c	69.2%

Note. Samples were taken 5 and 60 min after addition of the oxidants (there was a 20- to 30-minute equilibration period in the experimental buffer at 37°C prior to oxidant addition in these experiments as opposed to the 5-min equilibration period for all the other experiments). Data presented are the x ± S.D. of N = 5–15 separate determinations.

[a] nmol/10⁶ cells expressed as GSH equivalents.

[b] These measurements were made from a set of P388D₁ cells grown at a later time and obtained from a different source (ATCC; see Methods section). The untreated plus-glucose controls also had higher levels of GSH (5.18 ± 1.22 nmol/10⁶ cells; N = 6; 60-min sample) which were not significantly different from the plus-glucose diamide samples. Although it is unclear why the newer batch of P388D₁ cells had much higher (2–3X) levels of total GSH than the older cells used for the majority of these experiments, the new cells also exhibited the same actin polymerization response to the oxidants as demonstrated with the original cells in Fig. 2 (N = 4; data not shown).

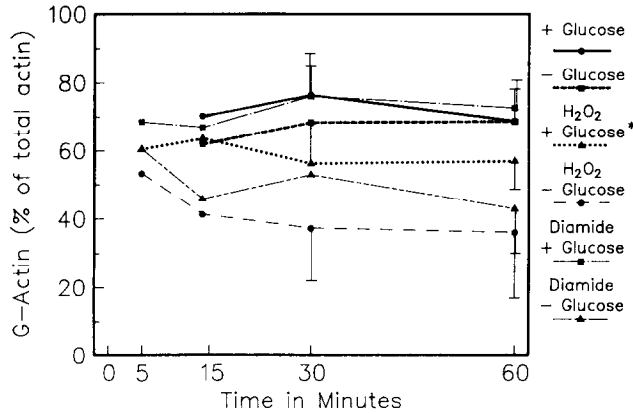[c] GSSG $< 1 \times 10^{-11}$ mol/10⁶ cells.

FIG. 1. The effect of H_2O_2 and diamide on actin in P388D$_1$ cells. Time course of actin polymerization (DNase I assay) following exposure to 5 mM H_2O_2 or 100 μM diamide $\pm$ glucose (5.5 mM). Each data point represents the x of N = four to eight separate determinations. Representative error bars for the standard deviation (SD) of individual means are also depicted. *Data for plus-glucose H_2O_2 have been previously published (see Ref. (3)) and are included here for completeness.

FIG. 2. Flow cytometric assay for polymerized (F) actin. P388D$_1$ cells were stained with NBD–phallacidin 60 min after exposure to 5 mM H_2O_2 or 100 μM diamide in the absence of glucose for comparison with control (uninjured) cells incubated in glucose (5.5 mM) for 60 min. Data are presented from a representative experiment repeated at least five times as an overlay of the plus-glucose control histogram (dotted trace) with the histograms for cells exposed to 5 mM H_2O_2 (solid trace) or 100 μM diamide (light trace) in the absence of glucose. The mean channel number for fluorescence of the H_2O_2-treated sample was 133.37 and of the diamide treated sample 162.41, 45.5, and 77.2% increases in F-actin, respectively, relative to the control (91.65, mean channel number for fluorescence).

course (Fig. 1; e.g., H_2O_2 minus-glucose vs H_2O_2 plus-glucose, P < 0.05). In contrast to H_2O_2, diamide only produced significant actin polymerization in P388D$_1$ cells when glucose was absent, which was also the condition necessary for the oxidant to cause GSSG formation (Table I). F-actin was also measured by flow cytometry of cells stained with NBD–phallacidin. A representative fluorescence histogram 60 min after oxidant exposure is depicted in Fig. 2 and confirms the observations in Fig. 1. Thus, it appeared that actin polymerization occurred only under conditions where significant sulfhydryl oxidation was present as indicated by the formation of GSSG.

P388D$_1$ cells were depleted of GSH by treatment with BSO prior to oxidant exposure. Treatment with BSO consistently reduced total cellular GSH to a level <1 $\times$ 10^{-11} mol/10^6 cells (approx. <1% of control, N = 11) without adverse effects on cellular viability (trypan blue exclusion > 90%). Figure 3 demonstrates the time course of actin polymerization in GSH-depleted cells following oxidant exposure. If GSH levels alone or the formation of GSSG were critical to the oxidant-induced actin polymerization, depletion of GSH should have prevented both the GSSG formation and the actin polymerization. Depletion of GSH did not stop the oxidant-induced polymerization of actin. Significant actin polymerization (P < 0.0001) was again seen only with the same conditions which produced it in Fig. 1, the only difference being a dramatic reduction in the pool of GSH available for oxidation, suggesting that the relevant targets are protein sulfhydryls. GSH depletion did significantly (P < 0.05) enhance the amount of actin polymerized in the minus-glucose diamide treated cells compared to their counterparts in Fig. 1 but did not significantly alter the pattern of actin polymerization induced by H_2O_2. Marked GSH
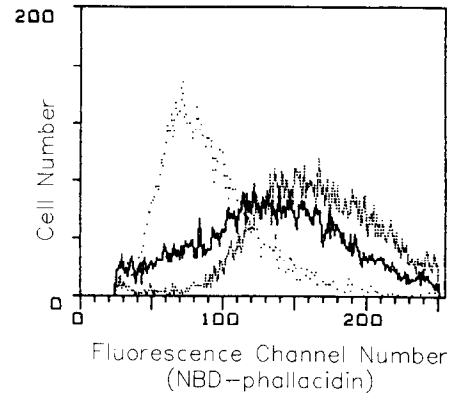
depletion induced by BSO treatment did not by itself induce actin polymerization in either the plus- or minus-glucose control. These results were also confirmed by the flow cytometric assay (data not shown).

ATP and Oxidant-Induced Actin Polymerization

Since our earlier observations (3, 4) demonstrated a close correlation between reduction of cellular ATP levels and disruption of microfilaments into bundles, we ex-
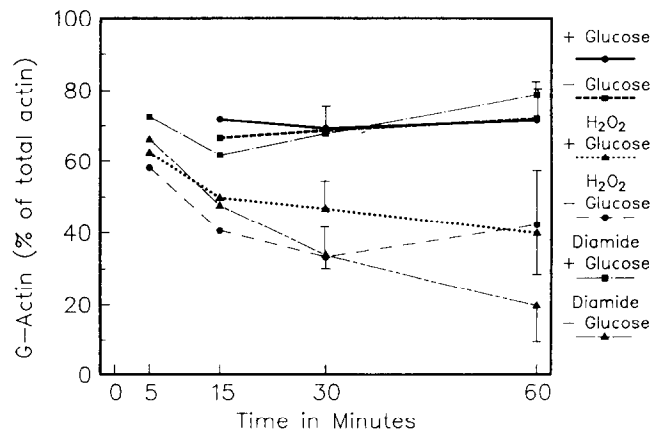

FIG. 3. The effect of H_2O_2 and diamide on actin in GSH depleted cells. Time course of actin polymerization (DNase I assay) following exposure to 5 mM H_2O_2 and 100 μM diamide $\pm$ glucose in BSO-treated cells. Each data point represents the x $\pm$ SD of N = 4–11 separate determinations.

amined the effect of the different conditions in our experiments on ATP levels in the P388D$_1$ cells (Fig. 4).

There were significant ($P < 0.05$) reductions of ATP levels seen with all of the conditions associated with formation of GSSG and actin polymerization in cells exposed to either oxidant. However, there was also a significant decline ($P < 0.05$) in ATP levels in cells deprived of glucose for 1 h, a condition which by itself was not associated with either GSSG formation or actin polymerization but was previously shown (3, 4) to be associated with disruption of microfilament organization and morphology. Thus, there was no direct correlation between ATP levels and the actin polymerization.

DISCUSSION

Conditions which caused the formation of GSSG and the oxidation of other sulfhydryl targets in P388D$_1$ cells were correlated with substantial actin polymerization measured by the DNase I assay and also confirmed by flow cytometry of cells stained with NBD–phallacidin. The approx. 10-fold higher percentage of GSSG in minus-glucose cells 5 min after treatment with H_2O_2 compared to plus-glucose cells exposed to H_2O_2 also correlated well with significantly greater amounts of actin polymerization during the 60-min time course. These observations suggest that the rate and extent of oxidant-induced polymerization of actin may directly depend on the pattern and extent of sulfhydryl oxidation occurring within injured cells.

Experiments in which cellular GSH was depleted with BSO pretreatment demonstrated that the oxidant-induced actin polymerization was not dependent on depletion of GSH or the formation of GSSG. GSH depletion did significantly enhance the effect of diamide on polymerization of actin but only when glucose was absent.

The demonstration of a marked loss (>95%) of GSH after BSO treatment alone without an associated increase in polymerized actin eliminated a direct role for GSH loss in the mechanism of oxidant-induced actin polymerization. It is interesting that depletion of GSH significantly enhanced the effect of diamide only on actin polymerization in minus-glucose cells. This may reflect differences in the specificity of the two oxidants for cellular targets. This observation also confirmed the earlier observation of increased platelet sensitivity to diamide after GSH depletion (16). The lack of actin polymerization in GSH-depleted cells exposed to 100 μM diamide in the presence of glucose suggests that P388D$_1$ cells may have an active enough HMP shunt to keep sulfhydryl targets reduced during diamide exposure even when cellular GSH levels are approx. 1% of normal, provided glucose is available.

Although ATP levels fell significantly in cells exposed to the oxidants under conditions leading to sulfhydryl oxidation and actin polymerization, reduction of ATP levels alone (e.g., minus-glucose control, Table I and Figs. 1 and 4) could not produce these effects. These observations indicate that additional pathologic changes involving the actin cytoskeleton occur during oxidative injury beyond the ATP-dependent changes in gross microfilament organization reported in earlier studies (3, 4). It would appear from these experiments that in addition to gross fragmentation of microfilament architecture which results from reduction of cellular ATP levels and does not involve actin polymerization, oxidant injury also induces a net assembly of actin within injured cells. The rate and extent of this polymerization of actin appears to correlate with the degree of sulfhydryl oxidation occurring in the injured cells.

In vitro studies of actin have demonstrated the presence of five sulfhydryl groups in the actin molecule which ex-
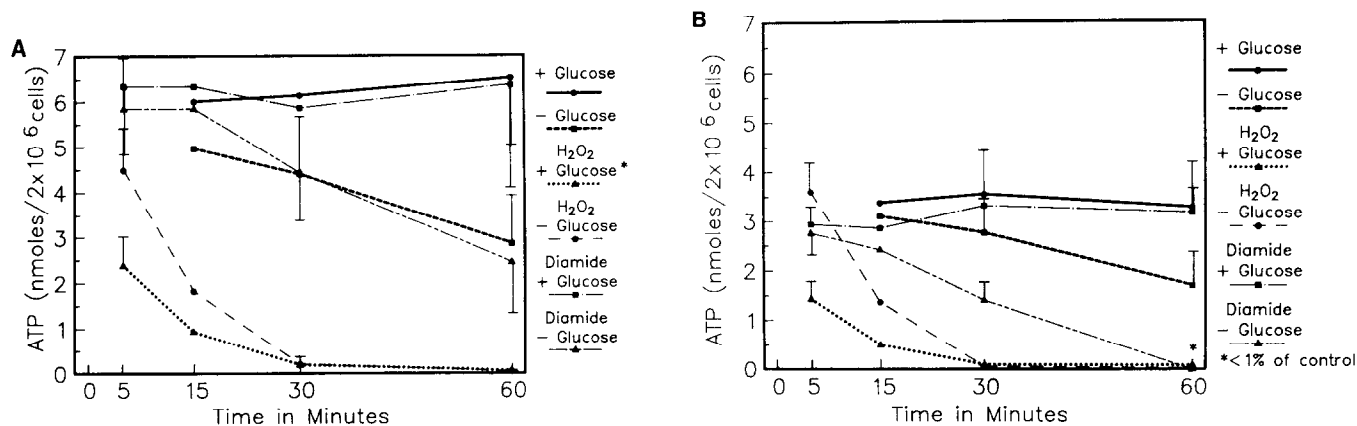

FIG. 4. The effect of H_2O_2 and diamide on ATP levels in P388D$_1$ cells. (A) Time course of ATP levels in P388D$_1$ cells following exposure to 5 mM H_2O_2 or 100 μM diamide ± glucose. Each data point represents the x of N = four to eight separate determinations. Representative error bars for the standard deviation (SD) of individual means are also depicted. *Data for plus-glucose H_2O_2 have been previously published (see Ref. (3)) and are included here for completeness. (B) Time course of ATP levels in P388D$_1$ cells depleted of GSH by prior BSO treatment following exposure to 5 mM H_2O_2 or 100 μM diamide ± glucose. Each data point represents the x ± SD of N = 4–11 separate determinations.

hibit variable reactivity to a number of sulfhydryl reactive agents, G-actin being more reactive than F-actin (24). Some of these agents inhibit actin polymerization while others (e.g., N-ethylmaleimide; NEM) enhance it or have no effect (24, 25). It has been postulated that the enhanced rate of polymerization of actin associated with some of the agents which bind to cysteine-373 in G-actin may be due to stabilization of actin nucleation sites thus overcoming the slow phase of actin assembly (25). We are currently examining the possibility that sulfhydryl oxidation may enhance the formation of actin nucleation sites within cells. The data presented here confirm and extend the earlier work of Wallace et al. (26) in which the sulfhydryl-reactive agent NEM increased F-actin in polymorphonuclear leukocytes as measured by increased binding of fluorescent phallotoxins. Work with polyacrylamide gel electrophoresis of the Triton X-100 insoluble extract from cells exposed to oxidants has demonstrated the presence of high molecular weight aggregates under nonreducing conditions which resolve in the presence of reducing agents like β-mercaptoethanol (1, 8–10). Mirabelli et al. have suggested that these aggregates contain sulfur cross-linked proteins including actin (8–10). It is not clear what relationship this phenomenon has to the actin polymerization demonstrated in this paper. The F-actin in oxidant injured cells depolymerized as readily as that in control cells when exposed to guanidine in the DNase I assay and total actin measured in either group was not significantly different (e.g., comparing cells depleted of GSH by BSO pretreatment: 15-min plus-glucose control = 2.53 ± 0.84 μg total actin/4×10^5 cells; $N = 11$ vs 15-min minus-glucose H_2O_2 = 2.56 ± 0.89 μg total actin/4×10^5 cells; $N = 7$). The DNase I assay was done under reducing conditions (0.5 mM DTT) which may account for the lack of difficulty in recovering total actin from the oxidant injured cells. The possibility exists that sulfhydryl oxidation might induce both phenomena, S-S cross-linking as well as regular actin assembly.

It thus appears that oxidant injury can initiate two separate events involving microfilaments: (i) an ATP-dependent disruption of gross microfilament structure into shortened bundles containing actin which does not require polymerization of actin (3) and (ii) assembly of actin polymers under conditions which induce oxidation of sulfhydryls within injured cells.

In summary, sulfhydryl oxidizing conditions induced actin assembly in P388D$_1$ cells. Sulfhydryl oxidation may be another pathway by which actin polymerization can be initiated within cells and may have particular relevance for understanding the mechanism of oxidant-mediated cellular injury.

REFERENCES

1. Hinshaw, D. B., Sklar, L. A., Bohl, B., Schraufstatter, I. U., Hyslop, P. A., Rossi, M. W., Spragg, R. G., and Cochrane, C. G. (1986) Am. J. Pathol. 123, 454–464.
2. Hinshaw, D. B., Burger, J. M., Armstrong, B. C., Hyslop, P. A. (1989) J. Surg. Res. 46, 339–349.
3. Hinshaw, D. B., Armstrong, B. C., Burger, J. M., Beals, T. F., and Hyslop, P. A. (1988) Am. J. Pathol. 132, 479–488.
4. Hinshaw, D. B., Armstrong, B. C., Beals, T. F., and Hyslop, P. A. (1988) J. Surg. Res. 44, 527–537.
5. Spragg, R. G., Hinshaw, D. B., Hyslop, P. A., Schraufstatter, I. U., and Cochrane, C. G. (1985) J. Clin. Invest. 76, 1471–1476.
6. Hyslop, P. A., Hinshaw, D. B., Halsey, W. A. Jr., Schraufstatter, I. U., Sauerheber, R. D., Spragg, R. G., Jackson, J. H., and Cochrane, C. G. (1988) J. Biol. Chem. 263, 1665–1675.
7. Schraufstatter, I. U., Hinshaw, D. B., Hyslop, P. A., Spragg, R. G., and Cochrane, C. G. (1985) J. Clin. Invest. 76, 1131–1139.
8. Mirabelli, F., Salis, A., Marinoni, V., Finardi, G., Bellomo, G., Thor, H., and Orrenius, S. (1988) Arch. Biochem. Biophys. 264, 261–269.
9. Mirabelli, F., Salis, A., Perotti, M., Taddei, F., Bellomo, G., and Orrenius, S. (1988) Biochem. Pharmacol. 37, 3423–3427.
10. Mirabelli, F., Salis, A., Vairetti, M., Bellomo, G., Thor, H., and Orrenius, S. (1989) Arch. Biochem. Biophys. 270, 478–488.
11. Jewell, S. A., Bellomo, G., Thor, H., Orrenius, S., and Smith, M. T. (1982) Science 217, 1257–1259.
12. Oliver, J. M., Albertini, D. F., and Berlin, R. D. (1976) J. Cell Biol. 71, 921–932.
13. Burchill, B. R., Oliver, J. M., Pearson, C. B., Leinbach, E. D., and Berlin, R. D. (1978) J. Cell Biol. 76, 439–447.
14. Nath, J., and Gallin, J. I. (1983) J. Clin. Invest. 71, 1273–1281.
15. Edelhauser, H. R., VanHorn, D. L., Miller, P., and Pederson, H. J. (1976) J. Cell Biol. 68, 567–578.
16. Bosia, A., Spangenberg, P., Ghigo, D., Heller, R., Losche, W., Pescarmona, G. P., and Till, U. (1985) Thrombosis Res. 37, 423–434.
17. Arrick, B. A., Nathan, C. F., Griffith, O. W., and Cohn, Z. A. (1982) J. Biol. Chem. 257, 1231–1237.
18. Griffith, O. W., and Meister, A. (1979) J. Biol. Chem. 254, 7558–7560.
19. Brehe, J. E., and Burch, H. B. (1976) Anal. Biochem. 74, 189–197.
20. Griffith, O. W. (1980) Anal. Biochem. 106, 207–212.
21. Blikstad, I., Markey, F., Carlsson, L., Persson, T., and Lindberg, U. (1978) Cell 15, 935–943.
22. Howard, T. H., and Meyer, W. H. (1984) J. Cell Biol. 98, 1265–1271.
23. Stanley, P. E., and Williams, S. G. (1969) Anal. Biochem. 29, 281–292.
24. Lusty, C. J., and Fasold, H. (1969) Biochemistry 8, 2933–2939.
25. Tait, J. F., and Frieden, C. (1982) Biochemistry 21, 6046–6053.
26. Wallace, P. J., Packman, C. H., Wersto, R. P., and Lichtman, M. A. (1987) J. Cell. Physiol. 132, 325–330.